◆ Human Brain Mapping 39:542–553 (2018) ◆

Differential Involvement of Nigral Subregions in Idiopathic Parkinson's Disease

Young Hee Sung,[1] Jongho Lee,[2] Yoonho Nam,[3] Hyeong-Geol Shin,[2] Young Noh,[1] Dong Hoon Shin,[1] and Eung Yeop Kim[4]*

[1]Department of Neurology, Gachon University Gil Medical Center, Incheon, South Korea
[2]Department of Electrical and Computer Engineering, Seoul National University, Seoul, Korea
[3]Department of Radiology, Seoul St. Mary's Hospital, College of Medicine, The Catholic University of Korea, Seoul, Korea
[4]Department of Radiology, Gachon University Gil Medical Center, Incheon, South Korea

Abstract: In this study, the prevalence of abnormality in putative nigrosome 1 and nigrosome 4 (N1 and N4, respectively) was investigated in early versus late-stage idiopathic Parkinson's disease (IPD) patients. A total of 128 IPD patients (early stage[$n = 89$]; late stage[$n = 39$]) and 15 healthy subjects were scanned for high-resolution ($0.5 \times 0.5 \times 1.0$ mm^3) multiecho gradient-recalled echo MRI and dopamine transporter PET imaging. The MRI data were processed for susceptibility map-weighted imaging (SMWI) to improve a contrast-to-noise ratio, and the images were resliced at 0.5 mm to define N1 and N4. When each side of N1 and N4 was assessed separately for the loss of hyperintensity by two independent reviewers, the consensus review results showed that in early-stage IPD (178 substantia nigras [SNs]), the loss of hyperintensity was observed more often in only the N1 region (65.2%) when compared to in both N1 and N4 regions (34.8%). In late-stage IPD (78 SNs), on the other hand, the loss in only the N1 region (25.6%) was less prevalent than in both N1 and N4 (74.4%) ($P < 0.0001$). Additionally, intact SNs (both in N1 and N4) were observed 17 SNs (9.6%) of the early-stage IPD patients, whereas it was not found in any SNs of the late-stage IPD patients ($P = 0.005$). Moreover, involvement of both N1 and N4 on both sides was found in 19.1% of the early-stage IPD patients, whereas its incidence was higher (61.5%) in the late-stage IPD patients ($P < 0.0001$), suggesting that the loss of hyperintensity in IPD progresses from N1 to N4 as the disease advances. *Hum Brain Mapp 39:542–553, 2018.* © 2017 Wiley Periodicals, Inc.

Key words: Parkinson disease; magnetic resonance imaging; substantia nigra; pars compacta; nigrosome

Additional Supporting Information may be found in the online version of this article.

Contract grant sponsor: Korea Healthcare Technology R&D Project through the Korea Health Industry Development Institute (KHIDI), funded by the Ministry of Health & Welfare, Republic of Korea; Contract grant numbers: HI17C1919; HI14C1135; Contract grant sponsor: Brain Research Program through the National Research Foundation of Korea (NRF), funded by the Ministry of Science, ICT & Future Planning; Contract grant number: NRF-2015M3C7A1031969

*Correspondence to: Eung Yeop Kim, MD; Department of Radiology, Gachon University Gil Medical Center, 21, Namdong-daero 774 beon-gil, Namdong-gu, Incheon 21565, South Korea. E-mail: neuroradkim@gmail.com

Received for publication 28 June 2017; Revised 8 October 2017; Accepted 17 October 2017.

DOI: 10.1002/hbm.23863

Published online 24 October 2017 in Wiley Online Library (wileyonlinelibrary.com).

INTRODUCTION

Idiopathic Parkinson's disease (IPD) is the most common cause of parkinsonism that is manifested by rest tremor, rigidity, bradykinesia, and postural instability. In patients with IPD, the number of pigmented neurons in the substantia nigra (SN) is reduced by 66% [Pakkenberg et al., 1991]. The SN is divided into two parts: the inferior and posterior SN pars compacta (SNpc) that contains melanized neurons, and the superior and anterior SN pars reticulata (SNpr). The neurons of the SNpc project to the striatum using the neurotransmitter dopamine. The neurons of the SNpr produce the neurotransmitter gamma-aminobutyric acid (GABA), and send axons to the thalamus. Approximately 60% of the neurons in the SNpc are lost by the time of symptomatic presentation [Hornykiewicz, 2006]. In its early stage of IPD, the ventrolateral portion of the substantia nigra (SN) is preferentially affected, resulting in the gradual loss of dopaminergic neurons in the SNpc [Porritt et al., 2005].

Within the SN, it has been reported that there are five calbindin-poor subregions, nigrosome 1–5 [Damier et al., 1999a]. In IPD, it has also been suggested that the loss of dopamine-containing neurons occurs most severely in the nigrosome 1, followed by the nigrosome 2, 4, 3, and 5, of which the nigrosome 5 is least affected [Damier et al., 1999b]. Recently, a study demonstrated loss of hyperintensity in the dorsal region of the SN in susceptibility-weighted imaging (SWI) in patients with IPD by using an ultra-high-field MRI [Kwon et al., 2012]. A subsequent histology–MRI correlation study showed that the hyperintense region in the dorsal SN in SWI matched to nigrosome 1 in histology and the hyperintensity is lost in IPD [Blazejewska et al., 2013]. Since these pioneering works, loss of nigral hyperintensity in SWI has recently emerged as a new imaging sign for idiopathic Parkinson's disease (IPD) [Bae et al., 2016; Cosottini et al., 2014, 2015; Gao et al., 2016; Kim et al., 2016; Mahlknecht et al., 2017; Noh et al., 2015; Oh et al., 2016; Oustwani et al., 2017; Reiter et al., 2015; Schwarz et al., 2014; Sung et al., 2016; Wang et al., 2017]. In these recent studies, researchers have assessed a subregion of the substantia nigra (SN), which is located in the posterior (or dorsal) aspect of the SN, to observe the presence or absence of hyperintensity in the subregion. This subregion has been referred to as "swallow tail" appearance [Gao et al., 2016; Oustwani et al., 2017; Schwarz et al., 2014; Wang et al., 2017], "dorsolateral nigral hyperintensity" [Reiter et al., 2015], "hyperintensity between two hypointense regions in the dorsal SN" [Cosottini et al., 2014, 2015; Frosini et al., 2016], "nigral hyperintensity" [Bae et al., 2016; Kim et al., 2016], and "nigrosome 1 region" [Blazejewska et al., 2013; Meijer et al., 2016; Nam et al., 2017; Noh et al., 2015; Oh et al., 2016; Sung et al., 2016].

In these previous studies, however, the nigrosome subregions were not specified despite the fact that nigrosome 1, 3, and 4 are located in the posterior aspect of the SN [Damier et al., 1999a]. Therefore, no study demonstrated if there is any differential involvement in each subregion of the nigrosome as the IPD progresses. The stage-dependent impairment of nigrosome subregions was also not described in the study of Damier et al [Damier et al., 1999b], which has a limited sample size (only five brains). A study demonstrated that an R2* map may reflect the progression of IPD, showing more impairment in the caudal SN in its late stage [Du et al., 2012]. As nigrosome 1, 3, and 4 are located in the dorsal SN and nigrosome 1 is more severely impaired in IPD, it may be hypothesized that these subregions may be differentially impaired according to the stage of IPD. That is, nigrosome 1 is first and more severely impaired in early-stage IPD, and nigrosome 4 and 3 are subsequently impaired, resulting in an increase of susceptibility in the dorsal SN.

Recently, a new method, susceptibility map-weighted imaging (SMWI), has been demonstrated to provide high-quality images of the SN with nigral hyperintensity in vivo at 3 T [Nam et al., 2017]. A recent study by taking advantage of high-resolution and high-field (9.4 T) ex vivo SWI images successfully identified all five nigrosome subregions [Massey et al., 2017]. With this information on the locations of each nigrosome subregion and by utilizing SMWI, we hypothesized that we may identify nigrosome 1, 3, and 4 separately in in vivo, thereby validating the histological outcomes of the previous study [Damier et al., 1999b] using a large number of in-vivo data, and we may also be able to test if there is any differential involvement of nigrosome subregions according to disease status. By conducting this study, we may not only validate the previous histological results of the limited sample size, but also obtain the information on the most affected region along with its precise location in MRI in IPD patients, which can help clinicians assess their patients. Hence, the purpose of this study was to identify the nigrosome regions in the dorsal SN of IPD patients and compare the prevalence of each affected nigrosome between early-stage and late-stage IPD.

MATERIALS AND METHODS

Participants

This study was approved by the Institutional Review Board. All participants of this study gave written informed consent. We enrolled consecutive 130 patients with IPD from our movement disorder clinic from November of 2014 to March of 2017. All patients underwent N-3-fluoropropyl-2-β-carbomethoxy-3-β-(4-iodophenyl)nortropane PET (FP-CIT PET) for the initial diagnosis at a PET/CT scanner (Biograph-6; Siemens). The detailed acquisition methods for FP-CIT PET were described elsewhere [Noh et al., 2015]. The clinical diagnosis was made by UK Parkinson's Disease Society Brain Bank Clinical Diagnostic Criteria [Hughes et al., 1992]. Hoehn and Yahr (H&Y) scales [Hoehn and

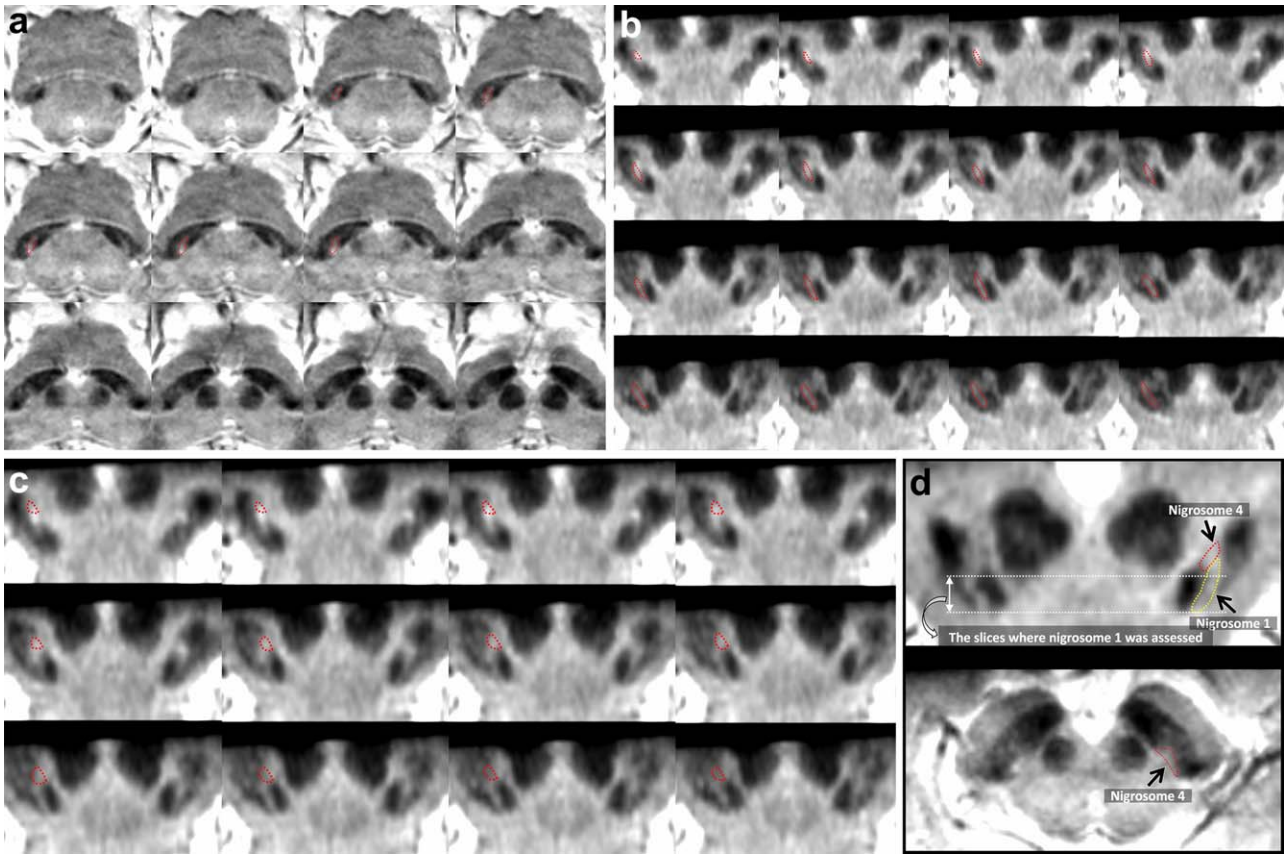

Figure 1.

A susceptibility map-weighted imaging (SMWI) of a 67-year-old healthy female. (**A**) SMWI obtained parallel to the line from the posterior commissure: upper border of the pons shows normal shape and location of the presumed nigrosome 1 regions (indicated with a dotted line) in the dorsal substantia nigra. (**B**) The reformatted SMWI perpendicular to the midbrain axis shows normal shape and location of the putative nigrosome 1 regions (indicated with a dotted line). The hyperintense region indicative of nigrosome 1 is mainly seen below the red nucleus. The arrows indicate the region of the decussation of the superior cerebellar peduncle. (**C**). The reformatted SMWI perpendicular to the midbrain axis shows normal shape and location of the putative nigrosome 4 regions (indicated with a dotted line), which is located in medial half of the substantia nigra at the level of lower 1/3 of the red nucleus. (**D**) Schematic drawing for the putative nigrosome 1 (yellow dotted line) and nigrosome 4 (red dotted line) regions. We assessed the nigrosome 1 below the red nucleus in this study. [Color figure can be viewed at wileyonlinelibrary.com]

Yahr, 1967] and Unified Parkinson Disease Rating Scale, Part I-III (UPDRS III) were recorded to evaluate the severity of motor symptoms by an experienced neurologist. The exclusion criteria for the diagnosis of IPD and the inclusion criteria for healthy subjects are summarized in Supporting Information.

As no histological validation was performed for the findings of the MRI results, we considered the findings on FP-CIT PET as a reference standard. Hence, decreased dopamine transporter activity in the basal ganglia on FP-CIT PET represented the presence of abnormality in the nigrosome 1 and/or nigrosome 4, whereas no abnormality on FP-CIT PET indicated that both the nigrosome 1 and nigrosome 4 were intact.

MR Image Acquisition

All participants underwent MR imaging at a 3 T scanner with a 32-channel coil (MAGNETOM Skyra; Siemens Healthineers, Forchheim, Germany). Whole-brain sagittal 3D MP-RAGE imaging was initially obtained with the following parameters: TR, 1800 ms; TE, 3 ms; TI, 920 ms; matrix 256 × 256; FOV, 250 × 250 (1-mm isovoxel); an acceleration factor of two; and acquisition time, 3:36 minutes. Oblique coronal three-dimensional multiecho combination imaging (MEDIC), which generates a combined image of multiecho gradient-recalled echo images, was obtained parallel to the plane from the posterior commissure and top of the pons, which was localized using

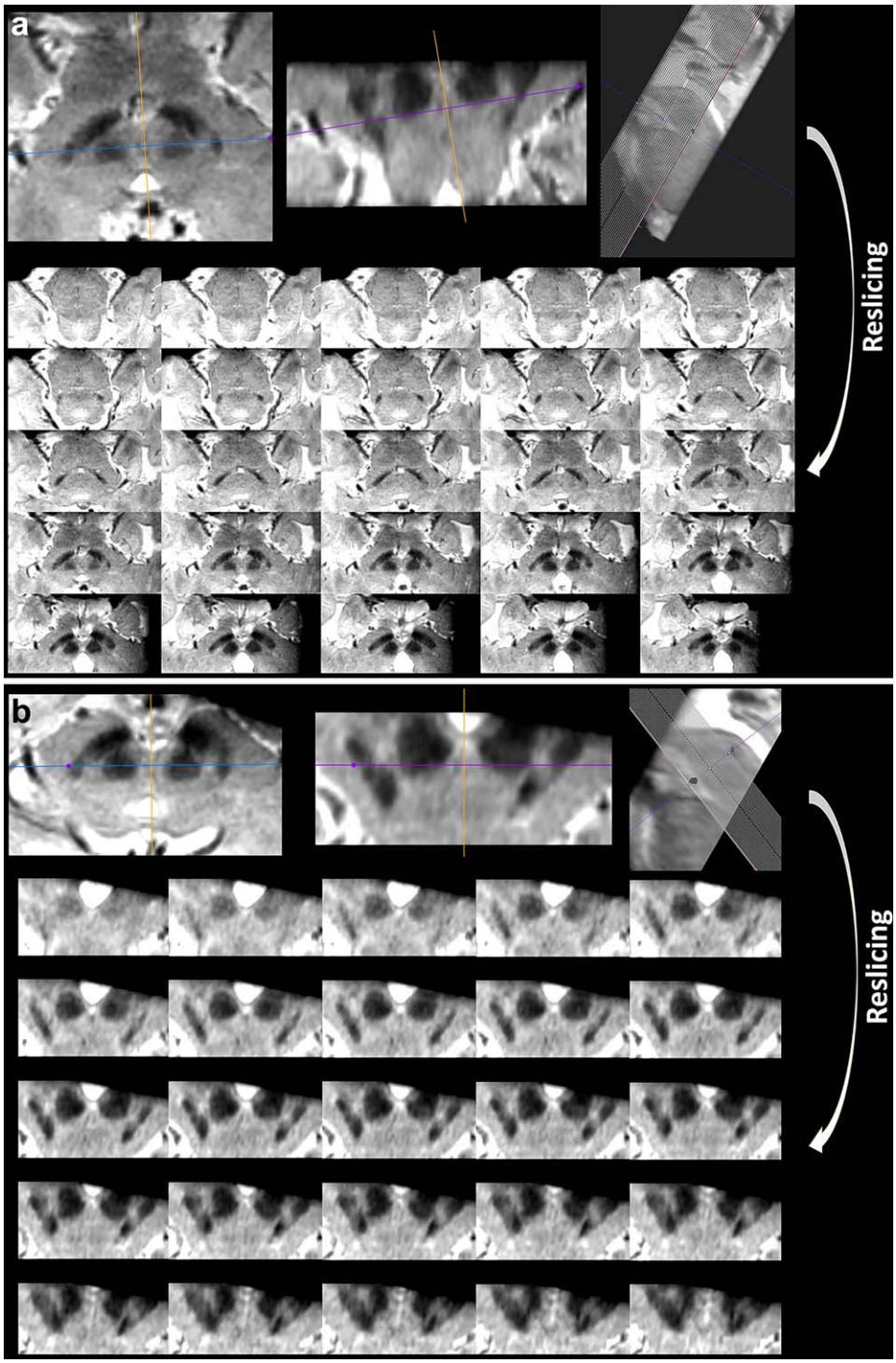

Figure 2.

Reslicing susceptibility map-weighted images when they are not obtained symmetrically, which are caused by various technical factors such as the patient's brain shape or inadvertent positioning. (**A**) SMWI of a 78-year-old female with early-stage IPD obtained parallel to the line from the posterior commissure: upper border of the pons was repositioned to be as symmetric as possible at the level of the lower border of the red nucleus, and thereafter the images were resliced at an increment of 0.5 mm. (**B**) The resliced images were reformatted perpendicular to the midbrain axis at an increment of 0.2 mm. (**C**) Although this was the most mal-aligned imaging in this study, it can determine abnormality in the bilateral nigrosome 1 regions (arrows; right more affected than left) below the red nucleus, when compared to their normal features in Figure 1A. Note the putative left nigrosome 4 region is normal, while right nigrosome 4 region is possibly abnormal (arrowheads). FP-CIT PET shows mild abnormality in the bilateral basal ganglia, right greater than left, which is well correlated with the findings on SMWI. [Color figure can be viewed at wileyonlinelibrary.com]

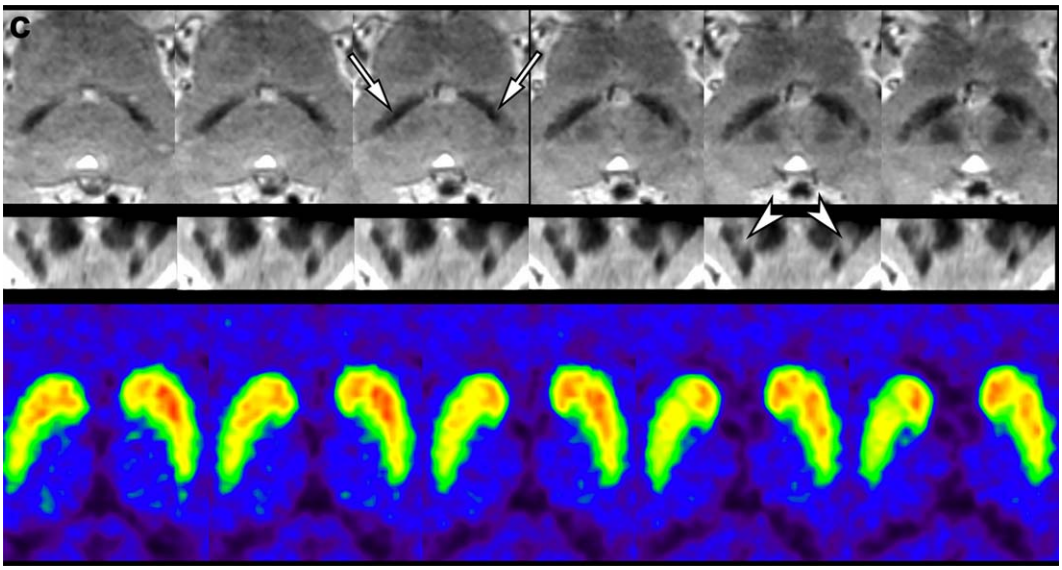

Figure 2.
(Continued). [Color figure can be viewed at wileyonlinelibrary.com]

the sagittal MP-RAGE images [Sung et al., 2016]. The scan parameters for MEDIC were as follows: TR, 88 ms; minimum TE, 11.1 ms; maximum TE, 66.9 ms; six echoes; echo spacing, 11.1 ms; flip angle, 10°; echo train length, six; thickness, 1 mm; number of sections, 28; 384 × 384 matrix; FOV, 192 × 192; acceleration factor of two; acquisition time, 7 min 19 s.

Definition of Nigrosome 1 and Nigrosome 4 on MRI for Visual Assessment

Based on the recent study by Massey et al. [2017], we defined the nigrosome 1 region as the central hyperintensity between two hypointense regions in the dorsal SN, which was assessed from the level of the anterior border of the red nucleus to the posterior end of the SN (Fig. 1A,B,D). As only a small part of the putative nigrosome 1 region exists at the level of lower 1/3 of the red nucleus [Massey et al., 2017], and it is less conspicuously identified than the rest of the putative nigrosome 1 region below the red nucleus (Fig. 1D), the latter region was only assessed for nigrosome 1 (hereafter, the putative nigrosome 1 region below the level of the red nucleus was designated as nigrosome 1). Unlike nigrosome 1 below the red nucleus, the border between nigrosome 4 and the putative nigrosome 1 was unclear at the level of lower one-third of the red nucleus on coronal-reformatted SMWI. Thus, we designated the hyperintense region located in the medial half of the SN at the level of lower one-third of the red nucleus on coronal-reformatted images (i.e., a craniomedial component of the dorsal nigral hyperintensity) as the putative nigrosome 4, and was assessed on coronal-reformatted images covering the anterior two-third of the red nucleus (Fig. 1C). Unfortunately, the nigrosome 3 was too small to be reliably identified in SMWI at 3 T and was not evaluated.

Reconstruction and Reslicing of Susceptibility Map-Weighted Imaging

The *k*-space data of the MEDIC scan were reconstructed for SMWI images using the procedure described by Nam et al. [2017]. This approach further enhances susceptibility contrast and helps to better visualize nigrosome structures.

The reconstructed SMWI data were resliced at an increment of 0.5 mm by using Syngo.via (version VA30, Siemens Healthcare, Germany). As not all the images were symmetric due to the head shape and/or position of the participants, they were repositioned as symmetric as possible at the level of the lower border of the red nucleus (Fig. 2A), which helped reviewers assess the nigrosome 1 (Fig. 2C). The resliced images were coronally reformatted perpendicular to the midbrain axis at an increment of 0.2 mm. This procedure helped to evaluate the nigrosome 4 (Fig. 2B).

Visual Assessment of Susceptibility Map-Weighted Imaging

A neuroradiologist and a neurologist independently reviewed images without any clinical information. The nigrosome 1 below the red nucleus on SMWI was considered "normal" when it maintains hyperintensity between the two hypointense regions (Fig. 1A and the right SN in Fig. 3); "possibly abnormal" when it loses hyperintensity <50% (the left SN of patient with the H&Y scale 1 in

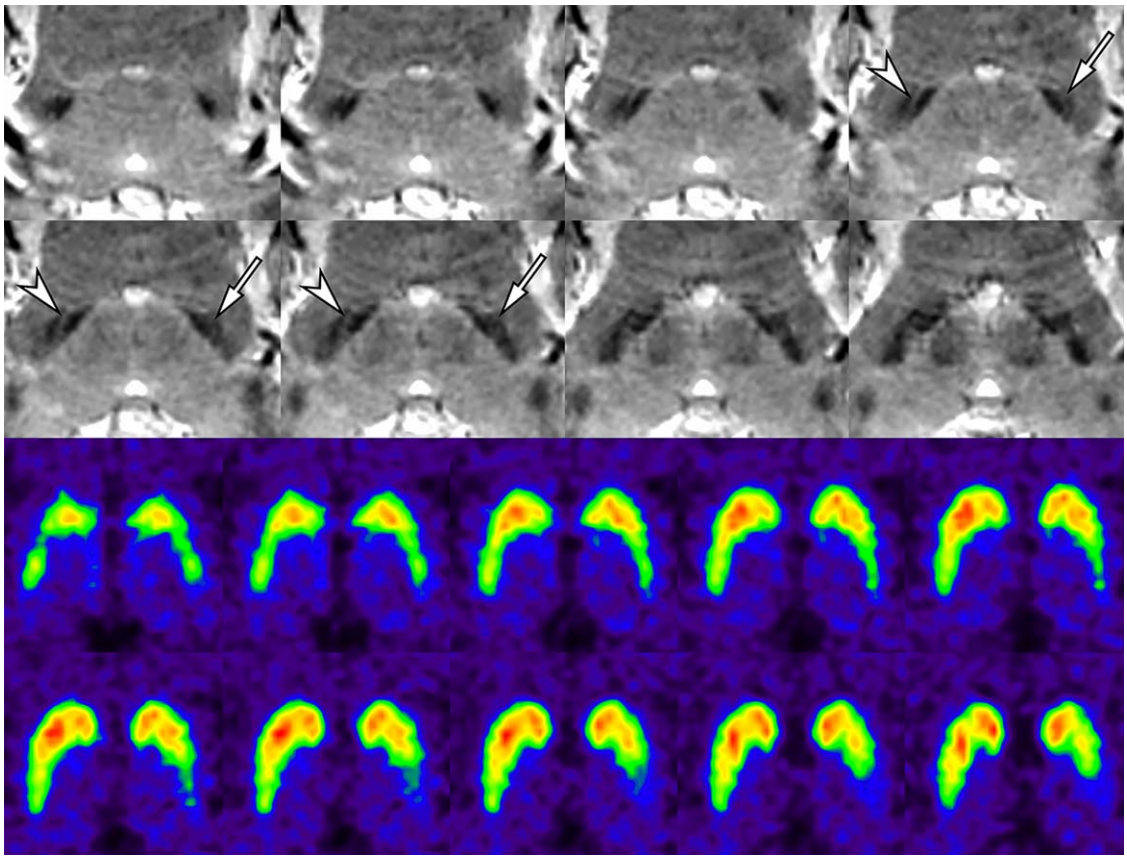

Figure 3.

False-negative interpretation for the putative nigrosome 1 region in a 58-year-old female with IPD (H&Y scale 1). The putative left nigrosome 1 region shows definite abnormality (arrows), whereas the right one maintains hyperintensity between the two adjacent hypointense regions (arrowheads). FP-CIT PET shows definite and mild abnormality in the left and right basal ganglia, respectively. [Color figure can be viewed at wileyonlinelibrary.com]

Fig. 4); and "definitely abnormal" when it is replaced by hypointensity equal to or more than 50% (the right SN of patient with the H&Y scale 1 in Fig. 4). The craniomedial component of dorsal nigral hyperintensity (putative nigrosome 4) was assessed in a similar fashion. Each side was rated separately. For simplifying statistical analysis, both "possibly "potentially abnormal" and "definitely abnormal" were lumped together as "abnormal." Any discrepancy between the two raters was resolved by consensus.

In addition to visual assessment of the dorsal nigral hyperintensity, the two independent reviewers were asked to draw regions of interest (ROIs) within the nigrosome 1 regions (Fig. 1A) and the putative nigrosome 4 regions (Fig. 1C) on the slice that most represented the presence or absence of signal alterations using commercial software, Analyze® (version 12.0, AnalyzeDirect, Overland Park, KS). Five healthy subjects and 30 patients with IPD (19 participants with early-stage IPD and 11 with late-stage IPD) were randomly chosen. Each side of the SN was evaluated separately. Each signal intensity of the nigrosome 1 and putative nigrosome 4 regions was divided by the signal intensity that was additionally measured in the region of the white matter at the level of the decussation of the superior cerebellar peduncle, which is typically located in the center of the midbrain at the level of the lowermost hypointensity (Fig. 1B). The average normalized signal intensity ratios between the two reviewers were compared between the intact and affected nigrosome regions that were determined by consensus reading. This procedure was conducted at least 1 month after the visual assessment to minimize recall bias, and was aimed to test interobserver agreement, particularly for the evaluation of the craniomedial component of dorsal nigral hyperintensity because of its arbitrary definition.

Visual Assessment of FP-CIT PET

A nuclear medicine specialist visually assessed FP-CIT PET without any clinical information. Striatal dopaminergic transporter activity was classified as normal or abnormal

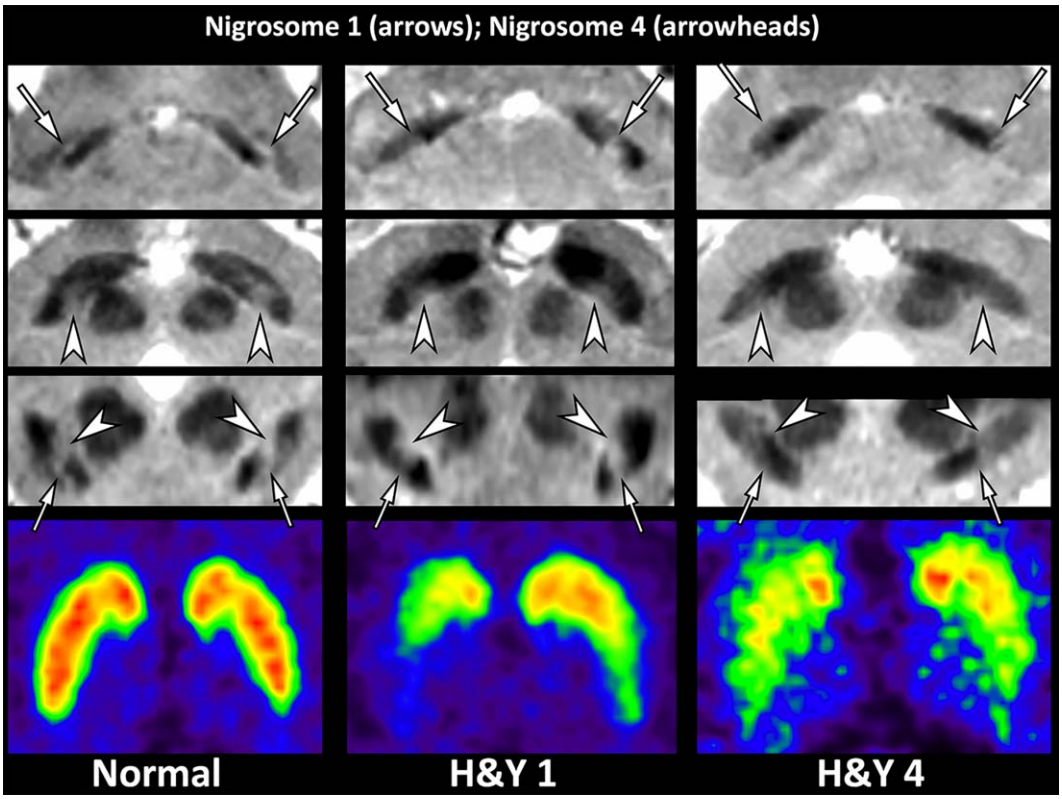

Figure 4.

Three representative participants including a 76-year-old healthy female, a 56-year-old female with early-stage IPD (Hoehn and Yahr scale 1), and a 79-year-old male with late-stage IPD (Hoehn and Yahr scale 4). The putative nigrosome 1 regions (arrows) are normal on both sides in the healthy subject, bilaterally abnormal (right more affected than left) in the patient with early-stage IPD, and bilaterally abnormal in the patient with late-stage IPD. The putative nigrosome 4 regions (arrowheads) are normal on both sides in both the healthy subject and the patient with early-stage IPD, whereas they are abnormal on both sides in the patient with late-stage IPD. These findings on SMWI are well correlated with those on FP-CIT PET. [Color figure can be viewed at wileyonlinelibrary.com]

grade I, II, and III according to the previous criteria [Benamer et al., 2000]. Normal activity was defined as bilateral symmetric tracer uptake in the putamina and caudate nuclei. Grade I abnormality was defined as asymmetric uptake with normal or almost normal putaminal activity on one side and with a more marked reduction in the contralateral side. Grade II was defined as significant reduction of activity in the bilateral putamina with preserved activity in the caudate nuclei. Grade III abnormality was defined as virtually absent uptake bilaterally in both the putamina and caudate nuclei. For simplifying statistical analysis, Grade I–III abnormalities were considered "abnormal." Each side of the basal ganglia was separately evaluated, and the presence or absence of abnormality of each side was recorded.

Statistical Analyses

Continuous variables were reported as mean ± standard deviation (SD) or median (interquartile range) according to the test results for normality. Categorical variables were compared by the Chi-square or Fisher's exact test as appropriate. Comparisons for continuous or ordinal variables were made with the Student *t*-test or Mann–Whitney *U* test as appropriate. Statistical comparisons were conducted between IPD patients and healthy subjects and between early-stage IPD (the H&Y scale ≤ 2) and late-stage IPD (the H&Y scale > 2) in terms of the prevalence of abnormality in the nigrosome 1 and/or the craniomedial component of dorsal nigral hyperintensity (putative nigrosome 4) per both the SN and participant. Statistical significance was set at $P < 0.05$. Statistical analyses were conducted with SPSS Statistics 23 (IBM, Armonk, NY).

RESULTS

Two of 130 patients (1.5%) with IPD showed severe motion-induced artifacts on MRI, and were excluded from further analysis. The median interval between FP-CIT PET

TABLE I. Demographic characteristics in study population

	IPD ($n = 128$)	Healthy subjects ($n = 15$)	Cohen's d	P value
Age	71.0 [65.0–76.0][a]	67.0 [63.0–68.5][a]	0.32	0.100[b]
Gender (female, %)	77 (53.8%)	10 (66.7%)	Not applicable	0.292[c]
Onset age (year)	68 [60.8–75.0][a]	Not applicable	Not applicable	
Disease duration (months)	12 [4.0–24.0][a]	Not applicable	Not applicable	
UPDRS I	2.0 [1.0–5.0][a]	Not applicable	Not applicable	
UPDRS II	7.5 [5.0–11.0][a]	Not applicable	Not applicable	
UPDRS III	18.0 [13–26.3][a]	Not applicable	Not applicable	
Hoehn & Yahr scale (1/1.5/2/2.5/3/4/5)	25/2/62/17/14/7/1	Not applicable	Not applicable	

[a]Data are median [interquartile range].
[b]Mann–Whitney *U* test.
[c]Chi-square test.

and SMWI MRI was 1 day (interquartile range, 0–7.5). After excluding these two participants, the SMWI images of 128 IPD patients and 15 healthy subjects were enrolled for visual assessment. Demographic and clinical characteristics of the participants are summarized in Table I.

In SMWI analysis of IPD patients, there was no false-positive interpretation. There were eight false-negative interpretations in nigrosome 1 of eight patients (the H&Y scale 1 [$n = 6$], scale 2 [$n = 1$], scale 2.5 [$n = 1$]); however, there was no bilateral false negative reading (i.e., at least one SN showed abnormality in the nigrosome 1 region in all early-stage and late-stage IPD patients). No abnormality was determined in nigrosome 1 or nigrosome 4 in 15 healthy subjects.

Table II shows the comparisons of the demographic data and prevalence of abnormality in nigrosome 1 and nigrosome 4 between patients with early-stage IPD (H&Y scale 1, 2) ($n = 89$) and those with late-stage IPD (H&Y scale 2.5–5) ($n = 39$). The patients with late-stage IPD were significantly older ($P = 0.001$), and had a longer disease duration ($P = 0.002$) and higher UPDRS I-III scores (all $P < 0.0001$).

Interobserver agreements for the visual assessment of right nigrosome 1, left nigrosome 1, right putative nigrosome 4, and left putative nigrosome 4 were all excellent with 0.929 (95% CI, 0.790–1.000), 0.905 (95% CI, 0.719–1.000), 0.950 (95% CI, 0.894–1.000), and 0.950 (95% CI, 0.894–1.000), respectively. In the randomly chosen 35 subjects, the consensus review

TABLE II. Comparison of demographic data and abnormality in nigrosome 1 and nigrosome 4 between early-stage IPD and late-stage IPD

Per patient analysis		Early-stage IPD patients ($n = 89$)	Late-stage IPD patients ($n = 39$)	Cohen's *d*	P value
Age		68.0 [62.−74.0][a]	75.0 [67.0–79.0][a]	0.70	0.001[b]
Gender (female, %)		48 (53.9%)	19 (48.7%)	Not applicable	0.587[c]
Onset age (year)		67.0 [59.0–73.0][a]	72.0 [64.0–77.5][a]	0.43	0.017
Disease duration (months)		12.0 [4.0–13.0][a]	24.0 [6.5–51.0][a]	0.67	0.002
UPDRS I		1.0 [1.0–4.0][a]	4.0 [2.0–7.0][a]	0.90	<0.0001[b]
UPDRS II		6.0 [4.0–8.0][a]	14.0 [10.0–18.0][a]	1.59	<0.0001[b]
UPDRS III		15.0 [12–19.0][a]	29.0 [23–38.5][a]	1.66	<0.0001[b]
Both nigrosome 1 and 4 affected in both SNs	No	72 (80.9%)	15 (38.5%)		<0.0001[c]
	Yes	17 (19.1%)	24 (61.5%)		

Per substantia nigra analysis	Substantia nigra of early-stage IPD ($n = 178$)	Substantia nigra of late-stage IPD ($n = 78$)	P value
Nigrosome 1 only affected	116 (65.2%)	20 (25.6%)	<0.0001[c]
Both nigrosome 1 and 4 affected	62 (34.8%)	58 (74.4%)	
Nigrosome 1 affected with or without nigrosome 4 affected	161 (90.4%)	78 (100%)	0.005[c]
Both nigrosome 1 and 4 intact	17 (9.6%)	0 (0%)	

[a]Data are median [interquartile range].
[b]Mann-Whitney *U* test.
[c]Chi-square test.

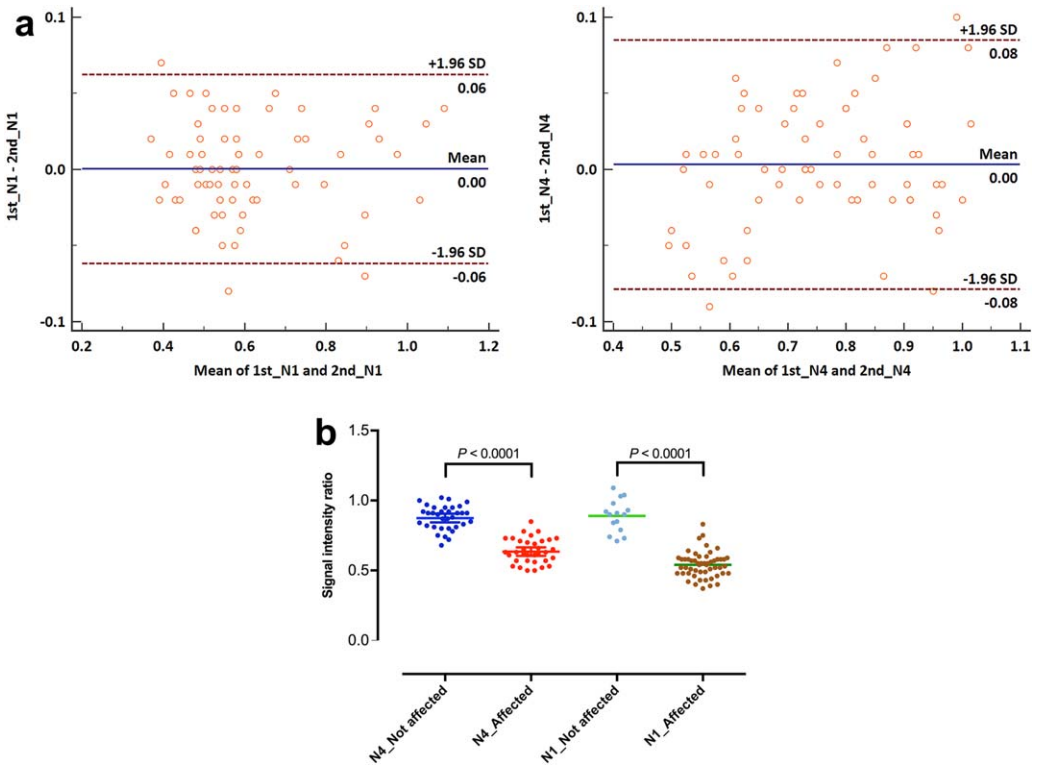

Figure 5.

Measurement of the signal intensity ratios in the nigrosome 1 region and the putative nigrosome 4 region in randomly selected 30 IPD patients and 5 healthy subjects (70 substantia nigras). (A) The Bland–Altman plots for measurement of the signal intensity ratios in the nigrosome 1 region (N1) and the putative nigrosome 4 region (N4) show that most measurements are within the upper and lower 95% limits of agreement (1st, the first reviewer; 2nd, the second reviewer). (**B**) The signal intensity ratios of the nigrosome 1 and putative nigrosome 4 regions are significantly different between the affected and not affected regions ($P < 0.0001$, both; Mann–Whitney *U* test). [Color figure can be viewed at wileyonlinelibrary.com]

determined 53 affected nigrosome 1 and 34 affected putative nigrosome 4. Intraclass correlation coefficients were 0.984 (95% CI, 0.974–0.990) for the nigrosome 1 region, and 0.961 (95% CI, 0.938–0.976) for the putative nigrosome 4 region. The Bland–Altman plot shows good agreement between the two reviewers (Fig. 5A). The normalized signal intensity ratios for the nigrosome 1 region were significantly different in both the nigrosome 1 region and putative nigrosome 4 region (median, 0.54 [0.48–0.58] for the affected nigrosome 1 region versus median, 0.90 [0.81–0.95] for the intact nigrosome 1 region; median, 0.63 [0.57–0.71] for the affected putative nigrosome 4 region versus median, 0.90 [0.82–0.94] for the intact putative nigrosome 4 region) ($P < 0.0001$, both) (Fig. 5B).

Isolated abnormality in nigrosome 1 was observed in 116 (65.2%) of 178 SNs of patients with early-stage IPD, whereas it was found in 20 out of 78 (25.6%) SNs of patients with late-stage IPD. While both nigrosome 1 and putative nigrosome 4 were affected in 62 SNs (34.8%) of patients with early-stage IPD, both were abnormal in 58 SNs (74.4%) of patients with late-stage IPD. As the putative nigrosome 4 was not solitarily affected, the ratios of the SNs with nigrosome 1 only affected to those with both nigrosome 1 and putative nigrosome 4 affected were significantly different between early-stage and late-stage IPD ($P < 0.0001$; Table II) (Fig. 6A). Both nigrosome 1 and putative nigrosome 4 were intact in 17 SNs of patients with early-stage IPD, whereas such observation was absent in those with late-stage IPD. All nigrosome 1 of the patients with late-stage IPD were abnormal along with or without abnormality in the putative nigrosome 4. The ratios of the SNs with both nigrosome 1 and putative nigrosome 4 intact to those with nigrosome 1 affected with or without nigrosome 4 affected were significantly different between early-stage and late-stage IPD ($P = 0.005$; Table II) (Fig. 6B). As at least one SN showed abnormality in the nigrosome 1 region in both early-stage and late-stage IPD patients and the putative nigrosome 4 was not solitarily affected in any SNs, we concluded that nigrosome 1 is more frequently affected in early-stage IPD, and then the putative nigrosome 4 is affected as the disease progresses. As expected, the proportion of patients with

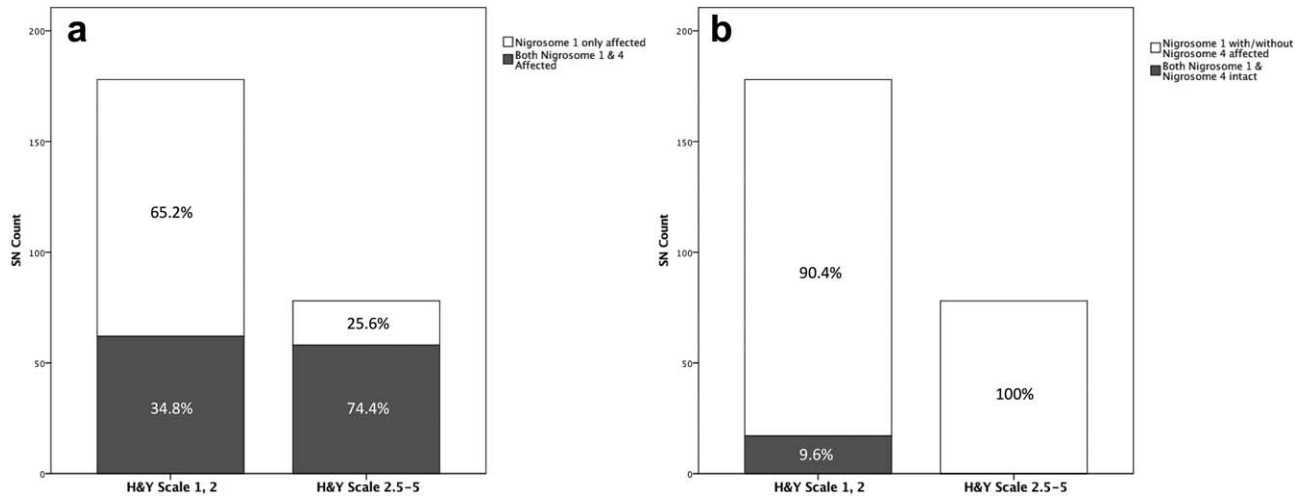

Figure 6.

Differential involvement of the putative nigrosome 1 and nigrosome 4 regions in IPD. (**A**) The ratios of the substantia nigra (SN) with isolated abnormality in the putative nigrosome 1 region to that with abnormality in both the putative nigrosome 1 and nigrosome 4 are significantly different between early-stage IPD and late-stage IPD. (**B**) The ratios of the SN with abnormality in the putative nigrosome 1 region with/without abnormality in the putative nigrosome 4 region to that without abnormality in both the putative nigrosome 1 and nigrosome 4 regions are significantly different between early-stage IPD and late-stage IPD.

abnormality in both nigrosome 1 and putative nigrosome 4 in both SNs was significantly higher in late-stage IPD than in early-stage IPD ($P < 0.0001$; Table II).

The statistical results above were not changed even when the eight IPD patients with false-negative interpretations on SMWI were excluded from the analysis or included as having unilateral abnormality in the nigrosome 1 of each patient.

DISCUSSION

The previous studies that evaluated the dorsal SN using SWI assessed the images at both the levels of the decussation of the superior cerebellar peduncle and the lower 1/3 of the red nucleus [Cosottini et al., 2014, 2015]. However, no study assessed nigrosome 1 and nigrosome 4 separately. By taking advantage of a high contrast-to-noise ratio (CNR) of SMWI along with a high spatial resolution ($0.5 \times 0.5 \times 1.0$ mm^3), we were able to identify both the nigrosome 1 and the putative nigrosome 4 regions at 3 T MRI. These regions are similar in terms of their shapes and locations to those in the previous histological study [Damier et al., 1999a] and the study at ultra-high-field MRI [Massey et al., 2017].

With improved anatomical localization, we observed that nigrosome 1 was more frequently affected than the putative nigrosome 4 in the early-stage IPD, whereas both subregions tended to be affected in the late-stage IPD. Our observations corroborate the previous pathological study by Damier et al. [1999b], where they demonstrated that the nigrosome 1 was the more severely affected than the nigrosome 4. In addition to validating the previous study results, our study suggested that the nigrosome 1 region is more vulnerable than the putative nigrosome 4 in the early-stage IPD by comparing the prevalence of abnormality in each region. We also showed that the evaluation of nigrosome 1 below the red nucleus was well associated with the ipsilateral side of dopaminergic transporter activity assessed by FP-CIT PET. Moreover, the ability to detect the subregions at clinically available 3T MRI may provide potential advantages of this approach for both initial diagnosis and assessing the severity of IPD patients.

Cosottini et al. [2014] suggested that the hyperintense region between the two hypointense regions in the dorsal SN is in the ventrolateral tier of the SNpc, which is reported to be the most vulnerable region for IPD [Fearnley and Lees, 1991]. This hyperintense region between the two hypointense regions in the dorsal SN appears as "swallow tail appearance" when an SWI image is obtained at the imaging plane parallel to the anterior commissure–posterior commissure line [Schwarz et al., 2014]. In other studies, the appearance of this hyperintense region was referred to as "dorsolateral nigral hyperintensity" [Reiter et al., 2015] or "nigral hyperintensity" [Bae et al., 2016]. These two studies obtained SWI at a relatively lower spatial resolution ($0.69 \times 0.92 \times 2.4$ mm^3 and $0.63 \times 0.63 \times 2.0$ mm^3, respectively) compared to those of other studies. As nigrosome 1 is located between the presumed dorsolateral tier of the SNpc and the presumed SNpr [Cosottini et al., 2014], and nigrosome 4 is located in the medial half of the dorsal SN [Massey et al., 2017], the designation "dorsolateral nigral hyperintensity" may be confusing.

Given that no SWI–pathological validation study per each nigrosome region with a sizable number of IPD patients has been performed, we believe that the designation of "dorsal nigral hyperintensity" may be more appropriate to indicate the nigrosome regions (specifically, nigrosome 1, 3, and 4) in the dorsal SN, particularly when SWI is obtained at a lower spatial resolution. With high-spatial-resolution SMWI, however, we may designate the most vulnerable region for IPD as "nigrosome 1 region" instead of "dorsal nigral hyperintensity."

Considering both our observations and the previous results [Massey et al., 2017], we may assert that the nigrosome 1 region needs to be assessed below the level of the red nucleus where the most of the region is identified with a higher contrast to the adjacent structures (the presumed dorsolateral tier of the SNpc and the presumed SNpr) irrespective of the imaging planes applied (see Supporting Information). Moreover, in our study, abnormality in the putative nigrosome 4 is always accompanied by ipsilateral abnormal nigrosome 1, while no abnormality in the putative nigrosome 4 does not necessarily mean intactness of nigrosome 1 on the same side. Nigrosome 4 is located at the level of lower part of the red nucleus, where it is in close proximity to nigrosome 1. Therefore, it may be appropriate to assess nigrosome 1 below the red nucleus on SWI or SMWI for proper prediction of presynaptic dopaminergic function.

Identification of the normal hyperintense nigrosome 1 region is very important because normal presynaptic dopaminergic function is currently one of the exclusion criteria for IPD [Postuma et al., 2015], and the preserved nigrosome 1 region in MRI can help predict normal presynaptic dopaminergic function [Bae et al., 2016]. In our study, only eight false-negative interpretations were observed for 8 IPD patients, but we were able to see abnormality in the contralateral nigrosome 1 regions in all of them without false-negative interpretation per patient. Compared to the previous results [Bae et al., 2016], we had improved diagnostic performance, which may be attributable to the new imaging method, SMWI, that has a higher contrast-to-noise ratio at a higher spatial resolution. However, it is necessary to note that only 15 healthy subjects were included in the study and our study did not intend to test the diagnostic power of SMWI. In addition, we did not enroll patients with atypical parkinsonism or others who present with parkinsonism, which is necessary to seek the clinical role of SMWI in real-world practice.

A previous study suggested that R2* of the SN, particularly in its caudal region, is strongly associated with disease progression [Du et al., 2012]. In their study, however, there was no further assessment for the nigrosome subregions. On the other hand, our study found that the putative nigrosome 4 region is more frequently affected along with involvement of ipsilateral nigrosome 1 in late-stage IPD. This observation may represent that the larger area of the dorsal SN turns hypointense in late-stage IPD, thereby partly explaining an increase of mean R2* in those patients. Nonetheless, the signal change in the nigrosome 1 region should be further assessed between early- and late-stage IPD to confirm the previous results.

This study has a few limitations as follows: first, we retrospectively assessed SMWI and FP-CIT PET although we had prospectively obtained them. Second, we only have indirect evidence that nigrosome 1 is more affected than the putative nigrosome 4 in early-stage IPD because the study is a cross sectional one. A longitudinal study may confirm our findings. Last, we do not have pathological validation for our observations, which may be more concerned for the definition of nigrosome 4 because nigrosome 1 and nigrosome 4 are in close proximity at the level of lower one-third of the red nucleus. Moreover, there is no definite anatomical border between them. Hence, we defined the putative nigrosome 4 region in the craniomedial component of the dorsal nigral hyperintensity. Although we showed excellent agreement for evaluating this region, further studies including imaging–pathological correlation may be necessary to confirm our observation. One may designate this region as "a craniomedial component of dorsal nigral hyperintensity" instead of the putative nigrosome 4 for more descriptive explanation.

CONCLUSION

In summary, we were able to evaluate nigrosome 1 and the putative nigrosome 4 separately at 3 T MRI using SMWI, and observed that differential involvement of them according to the stage of IPD (i.e., more frequent abnormality in nigrosome 1 than in the putative nigrosome 4 in early-stage IPD, more frequent abnormality in the putative nigrosome 4 in late-stage IPD than in early-stage IPD, and no solitary involvement of the putative nigrosome 4 in any SNs), which suggests sequential involvement of the putative nigrosome 4 as the disease progresses and may help clinicians where to assess on MRI to predict presynaptic dopaminergic function in early-stage IPD.

REFERENCES

Bae YJ, Kim JM, Kim E, Lee KM, Kang SY, Park HS, Kim KJ, Kim YE, Oh ES, Yun JY, Kim JS, Jeong HJ, Jeon B, Kim SE (2016): Loss of nigral hyperintensity on 3 Tesla MRI of Parkinsonism: Comparison with (123) I-FP-CIT SPECT. Mov Disord 31: 684–692.

Benamer TS, Patterson J, Grosset DG, Booij J, de Bruin K, van Royen E, Speelman JD, Horstink MH, Sips HJ, Dierckx RA, Versijpt J, Decoo D, Van Der Linden C, Hadley DM, Doder M, Lees AJ, Costa DC, Gacinovic S, Oertel WH, Pogarell O, Hoeffken H, Joseph K, Tatsch K, Schwarz J, Ries V (2000): Accurate differentiation of parkinsonism and essential tremor using visual assessment of [123I]-FP-CIT SPECT imaging: The [123I]-FP-CIT study group. Mov Disord 15:503–510.

Blazejewska AI, Schwarz ST, Pitiot A, Stephenson MC, Lowe J, Bajaj N, Bowtell RW, Auer DP, Gowland PA (2013):

Visualization of nigrosome 1 and its loss in PD: Pathoanatomical correlation and in vivo 7 T MRI. Neurology 81:534–540.

Cosottini M, Frosini D, Pesaresi I, Costagli M, Biagi L, Ceravolo R, Bonuccelli U, Tosetti M (2014): MR imaging of the substantia nigra at 7 T enables diagnosis of Parkinson disease. Radiology 271:831–838.

Cosottini M, Frosini D, Pesaresi I, Donatelli G, Cecchi P, Costagli M, Biagi L, Ceravolo R, Bonuccelli U, Tosetti M (2015): Comparison of 3T and 7T susceptibility-weighted angiography of the substantia nigra in diagnosing Parkinson disease. AJNR Am J Neuroradiol 36:461–466.

Damier P, Hirsch EC, Agid Y, Graybiel AM (1999a): The substantia nigra of the human brain. I. Nigrosomes and the nigral matrix, a compartmental organization based on calbindin D(28K) immunohistochemistry. Brain 122: 1421–1436.

Damier P, Hirsch EC, Agid Y, Graybiel AM (1999b): The substantia nigra of the human brain. II. Patterns of loss of dopamine-containing neurons in Parkinson's disease. Brain 122: 1437–1448.

Du G, Lewis MM, Sen S, Wang J, Shaffer ML, Styner M, Yang QX, Huang X (2012): Imaging nigral pathology and clinical progression in Parkinson's disease. Mov Disord 27:1636–1643.

Fearnley JM, Lees AJ (1991): Ageing and Parkinson's disease: Substantia nigra regional selectivity. Brain 114: 2283–2301.

Frosini D, Ceravolo R, Tosetti M, Bonuccelli U, Cosottini M (2016): Nigral involvement in atypical parkinsonisms: Evidence from a pilot study with ultra-high field MRI. J Neural Transm (Vienna) 123:509–513.

Gao P, Zhou PY, Wang PQ, Zhang GB, Liu JZ, Xu F, Yang F, Wu XX, Li G (2016): Universality analysis of the existence of substantia nigra "swallow tail" appearance of non-Parkinson patients in 3T SWI. Eur Rev Med Pharmacol Sci 20:1307–1314.

Hoehn MM, Yahr MD (1967): Parkinsonism: Onset, progression and mortality. Neurology 17:427–442.

Hornykiewicz O (2006): The discovery of dopamine deficiency in the parkinsonian brain. J Neural Transm Suppl 9–15.

Hughes AJ, Daniel SE, Kilford L, Lees AJ (1992): Accuracy of clinical diagnosis of idiopathic Parkinson's disease: A clinico-pathological study of 100 cases. J Neurol Neurosurg Psychiatry 55:181–184.

Kim JM, Jeong HJ, Bae YJ, Park SY, Kim E, Kang SY, Oh ES, Kim KJ, Jeon B, Kim SE, Cho ZH, Kim YB (2016): Loss of substantia nigra hyperintensity on 7 Tesla MRI of Parkinson's disease, multiple system atrophy, and progressive supranuclear palsy. Parkinsonism Relat Disord 26:47–54.

Kwon DH, Kim JM, Oh SH, Jeong HJ, Park SY, Oh ES, Chi JG, Kim YB, Jeon BS, Cho ZH (2012): Seven-Tesla magnetic resonance images of the substantia nigra in Parkinson disease. Ann Neurol 71:267–277.

Mahlknecht P, Krismer F, Poewe W, Seppi K (2017): Meta-analysis of dorsolateral nigral hyperintensity on magnetic resonance imaging as a marker for Parkinson's disease. Mov Disord 32: 619–623.

Massey LA, Miranda MA, Al-Helli O, Parkes HG, Thornton JS, So PW, White MJ, Mancini L, Strand C, Holton J, Lees AJ, Revesz T, Yousry TA (2017): 9.4 T MR microscopy of the substantia nigra with pathological validation in controls and disease. NeuroImage Clin 13:154–163.

Meijer FJ, Steens SC, van Rumund A, van Cappellen van Walsum AM, Kusters B, Esselink RA, Verbeek MM, Bloem BR, Goraj B (2016): Nigrosome-1 on susceptibility weighted imaging to differentiate Parkinson's disease from atypical Parkinsonism: An in vivo and ex vivo pilot study. Pol J Radiol 81:363–369.

Nam Y, Gho SM, Kim DH, Kim EY, Lee J (2017): Imaging of nigrosome 1 in substantia nigra at 3T using multiecho susceptibility map-weighted imaging (SMWI). J Magn Reson Imag 46: 528–536.

Noh Y, Sung YH, Lee J, Kim EY (2015): Nigrosome 1 detection at 3T MRI for the diagnosis of early-stage idiopathic Parkinson disease: Assessment of diagnostic accuracy and agreement on imaging asymmetry and clinical laterality. AJNR Am J Neuroradiol 36:2010–2016.

Oh SW, Shin NY, Lee JJ, Lee SK, Lee PH, Lim SM, Kim JW (2016): Correlation of 3D FLAIR and dopamine transporter imaging in patients with Parkinsonism. AJR Am J Roentgenol 207: 1089–1094.

Oustwani CS, Korutz AW, Lester MS, Kianirad Y, Simuni T, Hijaz TA (2017): Can loss of the swallow tail sign help distinguish between Parkinson Disease and the Parkinson-Plus syndromes? Clin Imag 44:66–69.

Pakkenberg B, Moller A, Gundersen HJ, Mouritzen Dam A, Pakkenberg H (1991): The absolute number of nerve cells in substantia nigra in normal subjects and in patients with Parkinson's disease estimated with an unbiased stereological method. J Neurol Neurosurg Psychiatry 54:30–33.

Porritt M, Stanic D, Finkelstein D, Batchelor P, Lockhart S, Hughes A, Kalnins R, Howells D (2005): Dopaminergic innervation of the human striatum in Parkinson's disease. Mov Disord 20:810–818.

Postuma RB, Berg D, Stern M, Poewe W, Olanow CW, Oertel W, Obeso J, Marek K, Litvan I, Lang AE, Halliday G, Goetz CG, Gasser T, Dubois B, Chan P, Bloem BR, Adler CH, Deuschl G (2015): MDS clinical diagnostic criteria for Parkinson's disease. Mov Disord 30:1591–1601.

Reiter E, Mueller C, Pinter B, Krismer F, Scherfler C, Esterhammer R, Kremser C, Schocke M, Wenning GK, Poewe W, Seppi K (2015): Dorsolateral nigral hyperintensity on 3.0T susceptibility-weighted imaging in neurodegenerative Parkinsonism. Mov Disord 30:1068–1076.

Schwarz ST, Afzal M, Morgan PS, Bajaj N, Gowland PA, Auer DP, Bush AI (2014): The 'swallow tail' appearance of the healthy nigrosome - a new accurate test of Parkinson's disease: A case-control and retrospective cross-sectional MRI study at 3T. PLoS One 9:e93814.

Sung YH, Noh Y, Lee J, Kim EY (2016): Drug-induced Parkinsonism versus idiopathic Parkinson disease: Utility of nigrosome 1 with 3-T imaging. Radiology 279:849–858.

Wang N, Yang H, Li C, Fan G, Luo X (2017): Using 'swallow-tail' sign and putaminal hypointensity as biomarkers to distinguish multiple system atrophy from idiopathic Parkinson's disease: A susceptibility-weighted imaging study. Eur Radiol 27: 3174–3180.